

Dynamic NMR and X-ray diffraction study of (N–B)-diphenyl(2-aminoethoxy) borane derivatives of ephedrine and pseudoephedrine

Herbert Höpfl^a, Norberto Farfán^{a,*}, Dolores Castillo^a, Rosa Santillan^a,
Rosalinda Contreras^a, Francisco Javier Martínez-Martínez^b, Marcelo Galván^c,
Rodolfo Alvarez^c, Lilia Fernández^d, Sabine Halut^e, Jean-Claude Daran^e

^a Departamento de Química, Centro de Investigación y de Estudios Avanzados del IPN, Apdo. Postal 14-740, 07000 México, D.F., México

^b Departamento de Química, Unidad Profesional Interdisciplinaria de Biotecnología-IPN, Av. Acueducto s/n, Barrio la Laguna Ticomán, 07340 México, D.F., México

^c Universidad Autónoma Metropolitana, Unidad Iztapalapa, Depto. Química, Apdo. Postal 55-534, 09340 México, D.F., México

^d Unidad Azcapotzalco, Av. San Pablo No. 180, Col. Reynosa Tamaulipas, México, D.F., México

^e Laboratoire de Chimie des Métaux de Transition, Université Pierre et Marie Curie, 4, Place Jussieu, Boite No. 42, 75252 Paris, Cedex 05, France

Received 5 November 1996; revised 17 February 1997

Abstract

The preparation and characterization of various (N–B)-diphenyl(2-aminoethoxy)boranes derived from ephedrine and pseudoephedrine derivatives (**1b–6b**) are reported: (N–B)-diphenyl(1-(*R*)-phenyl-2-(*S*)-methyl-2-aminoethoxy)borane (**1b**), (N–B)-diphenyl(1-(*R*)-phenyl-2-(*R*)-methyl-2-aminoethoxy)borane (**2b**), (N–B)-diphenyl[*N*-(*R*)-methyl-(1-(*R*)-phenyl-2-(*S*)-methyl-2-aminoethoxy)]borane (**3b-trans**), (N–B)-diphenyl[*N*-(*S*)-methyl-(1-(*R*)-phenyl-2-(*S*)-methyl-2-aminoethoxy)]borane (**3b-cis**), (N–B)-diphenyl[*N*-(*S*)-methyl-(1-(*R*)-phenyl-2-(*R*)-methyl-2-aminoethoxy)]borane (**4b-trans**), (N–B)-diphenyl[*N,N*-dimethyl-(1-(*R*)-phenyl-2-(*S*)-methyl-2-aminoethoxy)]borane (**5b**) and (N–B)-diphenyl[*N,N*-dimethyl-(1-(*R*)-phenyl-2-(*R*)-methyl-2-aminoethoxy)]borane (**6b**). The five membered N → B cyclic structures **1b–6b** were assigned based on ¹H-, ¹³C-, ¹¹B- and ¹⁵N-NMR data and all compounds except for **3b-trans** were subjected to X-ray diffraction analysis showing N → B bond lengths of 1.66(2) and 1.64(2) Å for **1b**, 1.657(9) and 1.664(9) Å for **2b**, 1.68(2) Å for **3b-cis**, 1.66(1) Å for **4b-trans**, 1.744(8) Å for **5b** and 1.74(1) Å for **6b**. The study of the intramolecular N → B coordination by means of dynamic NMR spectroscopy afforded ΔG^\ddagger values of 67.9, 70.9, 64.8, 68.2, 49.7 and 52.7 kJ mol⁻¹ for the dissociation of the N → B bond in compounds **1b–6b** respectively. The results show that steric interactions between the substituents at the (2-aminoethoxy)borane ring determine the stability of the N → B bond as well as the nitrogen configuration. Theoretical calculations of the electrostatic charges for the boron and nitrogen atoms in **1b**, **2b**, **3b-cis**, **3b-trans**, **4b-cis**, **5b** and **6b** show that the increase of positive charge on the nitrogen atom causes a shift to lower frequencies in the ¹⁵N NMR spectra. © 1997 Elsevier Science S.A.

1. Introduction

The work described in this paper continues our studies on the intramolecular N → B coordination with (N–B)-diphenyl(2-aminoethoxy)boranes derived from ephedrine and pseudoephedrine derivatives (**1b–6b**).

A different degree of methyl-substitution on the nitrogen atom permits a comparative study of the coordinative N → B bond within two series of compounds (**1b**, **3b**, **5b** and **2b**, **4b**, **6b**). Data obtained from kinetic,

theoretic and crystallographic measurements provide new insights into the stability of this bond that could be important for future applications of (2-aminoethoxy)boranes. The formation of (2-aminoethoxy)boranes has already been used in organic synthesis to increase the enantiomeric excess after hydroboration reactions (see for example Ref. [1]) and to separate diastereomeric and racemic methoxyborolane mixtures [2].

Previous studies concerning the determination of kinetic parameters for the dissociation of N → B coordinative bonds include data on intramolecular boronate-

* Corresponding author.

amines, borane amines and spiroborates derived from catecholborane and ephedrine-type aminoalcohols [3].

We have studied the molecular structures of dibenzobicyclic phenylboronates [4] and bicyclic phenylboronates derived from *N*-alkyl-*N*-(2-hydroxyethyl)glycines [5], as well as diphenylboronates derived from pyridylalcohols [6] by ^1H -, ^{13}C -, ^{11}B -NMR and X-ray diffraction analysis of single crystals.

More recently Toyota and Ōki reported the X-ray structure of 9-[2-dialkylaminomethylphenyl]-bora-bicyclo[3.3.1]nonanes [7] and proposed that the barrier of the dissociation for $\text{N} \rightarrow \text{B}$ bonds can be correlated with the tetrahedral character calculated from bond angles at the boron atom. In addition, Ferguson et al. [8] reported the equilibrium between four- and three-coordinate boron species, with the latter formed by scission of the $\text{N} \rightarrow \text{B}$ bond in borosilicates.

We have also been interested in the study of compounds containing chiral nitrogen of stable configuration obtained by nitrogen–boron coordination [9]. In these compounds the stereochemistry at the nitrogen atom can be deduced from the chemical shifts which are affected by steric hindrance [10,11]. The importance of chiral boron heterocycles in asymmetric synthesis is well documented [12–17].

2. Results and discussion

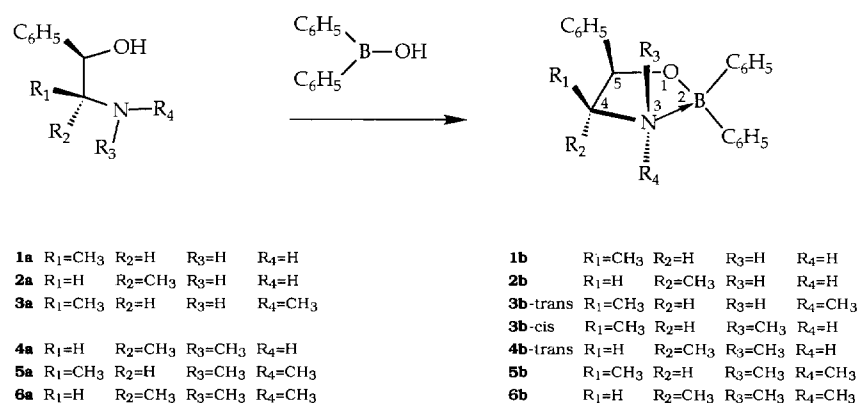
The preparation of (N–B)-diphenyl(1-(*R*)-phenyl-2-(*S*)-methyl-2-aminoethoxy)borane (**1b**), (N–B)-diphenyl(1-(*R*)-phenyl-2-(*R*)-methyl-2-aminoethoxy)borane (**2b**), (N–B)-diphenyl[*N*-(*R*)-methyl-(1-(*R*)-phenyl-2-(*S*)-methyl-2-aminoethoxy)]borane (**3b-trans**), (N–B)-diphenyl[*N*-(*S*)-methyl-(1-(*R*)-phenyl-2-(*S*)-methyl-2-aminoethoxy)]borane (**3b-cis**), (N \rightarrow B)-diphenyl[*N*-(*S*)-methyl-(1-(*R*)-phenyl-2-(*R*)-aminoethoxy)]borane (**4b-trans**), (N–B)-diphenyl[*N,N*-dimethyl-(1-(*R*)-phenyl-2-(*S*)-methyl-2-aminoethoxy)]-

borane (**5b**), and (N–B)-diphenyl[*N,N*-dimethyl(1-(*R*)-phenyl-2-(*R*)-methyl-2-aminoethoxy)]borane (**6b**) was achieved by reaction of the corresponding aminoalcohol with diphenylborinic acid (Scheme 1).

The ^1H NMR, ^{13}C - and ^{11}B -NMR chemical shifts of **1b–6b** are listed in Tables 1 and 2 respectively. Formation of cyclic structures can be easily demonstrated by spectroscopic methods since the ^{11}B NMR chemical shifts (Table 2) lie in the range corresponding to $\text{N} \rightarrow \text{B}$ coordination compounds [3–6]. It is interesting to note that in contrast to $\text{N}-\text{BH}_3$ adducts of ethanolamines [10], the ^{11}B NMR chemical shifts of (N–B)diphenyl(2-aminoethoxy)boranes are only slightly affected by substituents at the nitrogen atom.

Examination of the data in Table 2 shows that the ^{13}C NMR chemical shift of C_5 corresponds to values between 76.3–78.4 ppm in ephedrine derivatives while the same carbon is in the range of 80.5–83.0 ppm in pseudoephedrine derivatives. The aromatic carbon signals of the diphenylboryl groups show constant chemical shifts and can be assigned based on multiplicity and comparison with similar compounds. The ipso-to-boron carbon atoms are observed in all cases as broad signals in the range of 147–151 ppm, the ortho carbon atoms appear around 131–133 ppm and the meta and para carbon atoms between 126–129 ppm. All (N–B)-diphenyl(2-aminoethoxy)boranes show diastereotopic signals for the two *B*-phenyl groups due to the existence of asymmetric carbons in the ephedrine and pseudoephedrine derivatives.

The *N*-methyl groups in the ^{13}C NMR spectra of **5b** and **6b** are observed as single signals at room temperature. However, at low temperatures, the same carbon atoms give rise to two signals. Assignment of each of the methyl signals was based on the greater steric congestion present for the *N*-methyl *cis* to *C*-methyl with a concomitant stronger γ -gauche effect. In contrast, the methyl group *trans* to *C*-methyl appears at lower field. A comparison with the ^{13}C NMR data of the analogous compounds **7** and **8** is presented in Scheme 2



Scheme 1. Reactions for the preparation of compounds **1b–6b**.

Table 1
¹H NMR data of (N-B)-diphenyl(2-aminoethoxy)boranes **1b–6b** in CDCl₃

Compound	C ₄ -CH ₃	N-CH ₃	NH	H ₄	H ₅	C ₆ H ₅
1b	0.62 (d) <i>J</i> = 6.6 Hz	—	3.86	3.28 (m)	4.98 (d) <i>J</i> = 5.3 Hz	7.15–7.57
2b	1.12 (d) <i>J</i> = 6.6 Hz	—	4.12	3.00 (m)	4.49 (d) <i>J</i> = 9.2 Hz	7.19–7.56
3b-trans	0.83 (d) <i>J</i> = 6.6 Hz	2.53 (s)	3.90	3.48 (m)	5.49 (d) <i>J</i> = 5.9 Hz	7.09–7.65
3b-cis ^a	0.83 (d) <i>J</i> = 6.6 Hz	2.22 (s)	6.85 (m)	3.15 (m)	4.95 (d) <i>J</i> = 6.0 Hz	7.09–7.65
4b-trans	1.05 (d) <i>J</i> = 6.6 Hz	2.28 (d) <i>J</i> = 5.9 Hz	3.66	2.65 (m)	4.44 (d) <i>J</i> = 9.2 Hz	7.15–7.66
4b-cis ^a	1.05 (d) <i>J</i> = 6.6 Hz	2.10 (d) <i>J</i> = 5.9 Hz	—	3.52 (m)	4.80 (d) <i>J</i> = 9.5 Hz	7.15–7.66
5b	0.78 (d) <i>J</i> = 7.3 Hz	2.38 (s)	—	3.40 (m)	5.64 (d) <i>J</i> = 7.9 Hz	7.15–7.53
6b	0.95 (d) <i>J</i> = 6.6 Hz	2.40 (s)	—	3.20 (m)	4.81 (d) <i>J</i> = 9.9 Hz	7.16–7.86

^a DMSO-*d*₆.

[2,10,11]. The ¹³C NMR chemical shifts of the methyl groups in **3b-trans**, **3b-cis** and **4b-trans** follow the same trends as those of the spiroborates **9-trans**, **9-cis**, and **10** (Scheme 3) [3].

In DMSO-*d*₆, nitrogen coordination to boron also gives rise to diastereotopic signals of the NH groups in the ¹H NMR spectra of **1b** and **2b**. Their assignment was verified by a HETCOR ¹⁵N-¹H NMR experiment for **1b** (Fig. 1).

The reaction of diphenylborinic acid with ephedrine

afforded the two N-epimers **3b-trans** and **3b-cis** (Scheme 1), whereas pseudoephedrine yields mainly **4b-trans**. The ephedrine epimer **3b-trans** can be isolated in pure form from chloroform; however, pure **3b-trans** equilibrates in DMSO to the epimeric mixture (**3b-trans**/**3b-cis**; *K* = 1.7, $\Delta G^\circ = -1.3 \text{ kJ mol}^{-1}$). The same phenomenon is observed for **4b-trans** which is also obtained pure from chloroform solutions (**4b-trans**/**4b-cis**; *K* = 19, $\Delta G^\circ = -7.1 \text{ kJ mol}^{-1}$).

In all cases the *N*-methyl or the *N*-hydrogen groups

Table 2
¹³C- and ¹¹B-NMR data of (N-B)-diphenyl(2-aminoethoxy)boranes **1b–6b** in CDCl₃

Compound	C-CH ₃	R ₃	R ₄	C ₄	C ₅	C-C ₆ H ₅ ipso	C-C ₆ H ₅ ortho	C-C ₆ H ₅ meta	C-C ₆ H ₅ para	B-C ₆ H ₅ ipso	B-C ₆ H ₅ ortho	B-C ₆ H ₅ meta	B-C ₆ H ₅ para	¹¹ B
1b	16.0	—	—	54.4	77.9	140.1	126.3	128.2	127.2	148.9 149.7	132.4 131.4	127.8 127.6	126.3 126.6	+7.4
2b	16.3	—	—	59.1	83.0	140.8	127.8	128.6	128.1	149.4	132.3 131.4	127.6 127.0	126.3 126.7	+7.0
3b-trans	13.4	34.4	—	61.7	78.4	141.0	126.7	127.4	126.4	148.0	133.0 131.9	128.3	127.6	+5.0
3b-cis ^b	9.6	32.8	—	59.0	76.3	141.3	—	—	—	151.0	130.9 132.6	126.6	128.0	—
4b-trans	13.7	36.8	—	68.0	81.7	140.8	126.9	127.6	128.1	—	133.8 131.2	127.9 127.3	128.8 126.4	+8.0
5b	9.6	44.0 41.9 ^c	44.0 45.5 ^c	65.2	76.7	141.6	127.1 ^a	127.2 ^a	128.3	147.6	131.9 133.2 131.1 ^d 133.4 ^d	128.0 127.4	126.6 126.0	+5.5
6b	8.9	44.4 47.3 ^c	44.4 41.9 ^c	69.4	80.5	141.2	127.5	128.5	126.3	147.6	133.4 133.5 ^e 132.1 ^e	127.2	128.0	+9.6

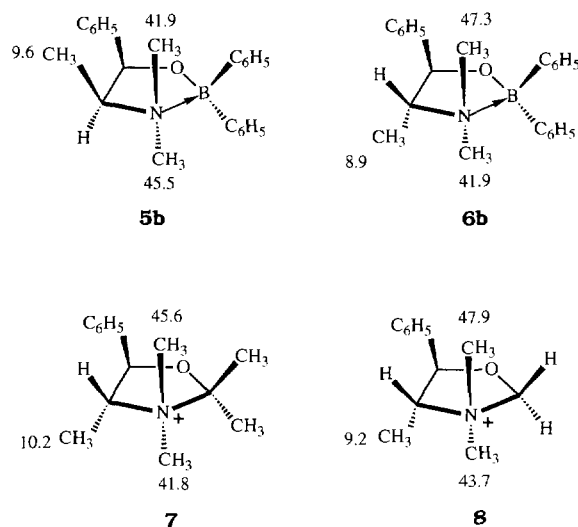
^a Signals may be interchanged.

^b In DMSO-*d*₆.

^c *N*-Methyl signals at -50 °C.

^d C(ortho)-B-Ph signals at -50 °C.

^e C(ortho)-B-Ph signals at -40 °C.



Scheme 2. Comparison of the ^{13}C NMR shifts between compounds **5b/7** and **6b/8**.

were used for the dynamic NMR study of the dissociation of the $\text{N} \rightarrow \text{B}$ bond. Studies of Toyota and Ōki have shown that the corresponding data of ^1H - and ^{13}C -NMR experiments are equivalent [3]. The ΔG^\ddagger data were derived from coalescence experiments and are compiled in Table 3.

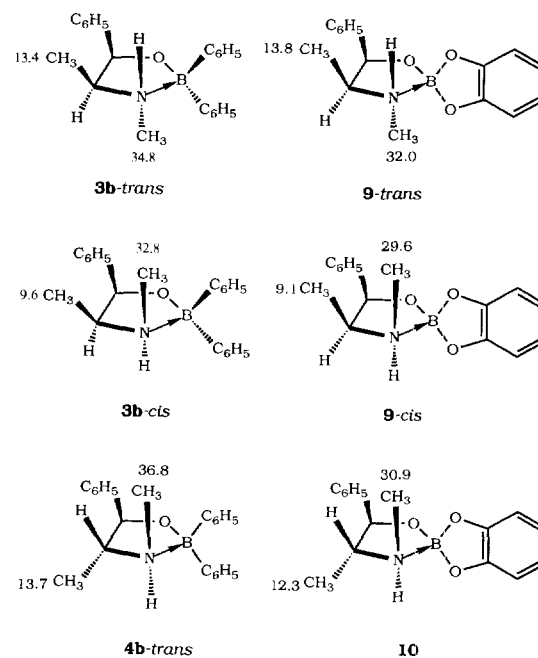
The dynamic process is shown graphically in Scheme 4. The dynamic process consists of four steps: $\text{N} \rightarrow \text{B}$ bond dissociation, rotation about the $\text{C}-\text{N}$ bond, inversion of the nitrogen atom and recoordination of the $\text{N} \rightarrow \text{B}$ bond [3].

The dissociation processes of the $\text{N} \rightarrow \text{B}$ bond show that pseudoephedrine derivatives **2b**, **4b** and **6b** are more stable than the corresponding ephedrine derivatives **1b**, **3b** and **5b**, in agreement with the fact that the *trans*-arrangement of the *C*-phenyl and *C*-methyl group gives a more stable ring. The major factor contributing to the destabilization of the *cis* isomer is probably due to the interaction of the substituents that are at a torsion angle lower than 52° (Table 16). The corresponding energy differences are 3.0 kJ mol^{-1} for **1b/2b**, 3.4 kJ mol^{-1} for **3b/4b** and 3.0 kJ mol^{-1} for **5b/6b**.

The $\Delta G_{\text{R1-N-R2}}^\ddagger$ values for **5b** and **6b** are lower than those of the corresponding catechol derivatives (**11**, 68.0 kJ mol^{-1} and **12**, 80.2 kJ mol^{-1} , Scheme 5) [3].

A comparison of the ΔG^\ddagger values of the ($\text{N}-\text{B}$)-diphenyl(2-aminoethoxy)boranes derived from ephedrine (**1b** > **3b** >> **5b**) and pseudoephedrine (**2b** > **4b** >> **6b**)¹ indicates that the less substituted nitrogen atoms give the stronger bonding due to differences in basicity and

¹ It has to be considered that there also exists a solvent effect, which lowers the ΔG^\ddagger values when changing from $\text{DMSO}-d_6$ to CDCl_3 . This difference should be significantly less than the observed changes in the compounds studied here [3].



Scheme 3. Comparison of the ^{13}C NMR shifts between compounds **3b-trans/9-trans**, **3b-cis/9-cis** and **4b-trans/10**.

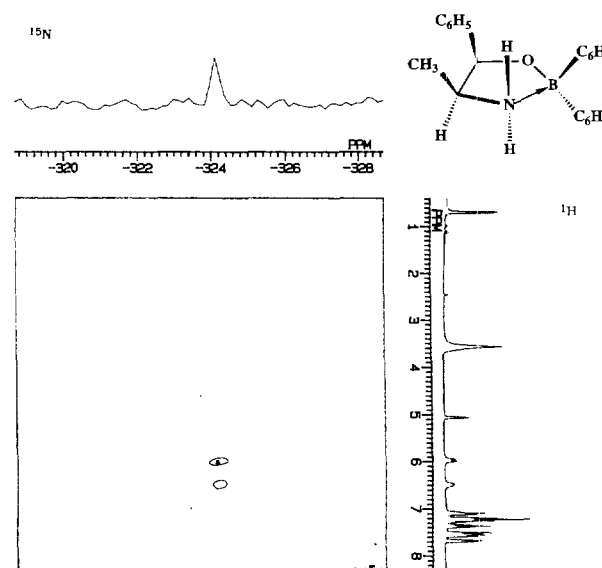


Fig. 1. $^1\text{H}-^{15}\text{N}$ HETCOR spectrum of **1b** ($\text{DMSO}-d_6$).

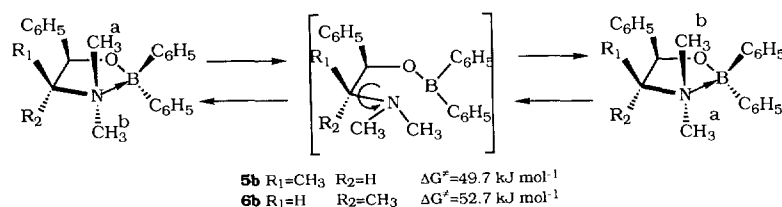
Table 3
 ΔG^\ddagger values^c for compounds **1b–6b** obtained from ^1H - and ^{13}C -NMR coalescence experiments

Compound	$\Delta G_{\text{R1-N-R2}}^\ddagger$ (kJ mol^{-1}) dissociation process
1b	67.9 ^a
2b	70.9 ^a
3b-trans	64.8 ^a
4b-trans	68.2 ^a
5b	49.7 ^b
6b	52.7 ^b

^a $\text{DMSO}-d_6$.

^b CDCl_3 .

^c The error is about 1.0 kJ mol^{-1} according to Ref. [18].

Scheme 4. Dissociation process due to an interchange of the *N*-methyl groups.

steric effects. The energy difference ($\Delta\Delta G_{R_1-N-R_2}^\ddagger$) between **1b** and **3b-trans** is 3.1 kJ mol^{-1} and the energy difference between **2b** and **4b-trans** is 2.7 kJ mol^{-1} .

^{15}N NMR measurements (Table 4) show that the nitrogen chemical shifts of the (N-B)-diphenyl(2-aminoethoxy)boranes are displaced about 20 ppm to higher frequencies with respect to the free aminoalcohols (**1a**, **3a**, **5a**). The ephedrine derivatives (**1b**, **3b**) are shifted a few parts per million upfield with respect to the pseudoephedrine derivatives (**3b**, **4b**).

The ^{15}N NMR shifts also show that α -effects in the (N-B)-diphenyl(2-aminoethoxy)boranes due to *N*-methyl substitution induce small shifts ($< 5 \text{ ppm}$) to lower frequencies, while the free aminoalcohols (**1a**, **3a** and **5a**) remain fairly constant. Small effects are observed due to a change in the configuration at C_4 .

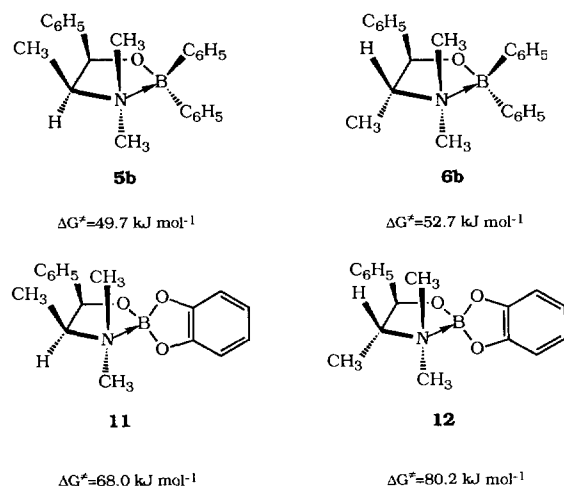
The shift to higher frequencies by the coordination to the boron atom can be attributed to electron density donation from the nitrogen to the boron atom. The loss of the labile nature of the N–H bond by nitrogen coordination to boron is also deduced from the N–H coupling, as the J_{NH} values lie in the range of $sp^3\text{-N}$ atoms [19].

The $\Delta G_{R_1-N-R_2}^\ddagger$ values of compounds **1b–4b** are correlated to the ^{15}N NMR chemical shifts δ (Eq. (1)).

$$\Delta G_{R_1-N-R_2}^\ddagger = 405.63 + 1.04\delta(^{15}\text{N NMR}) \quad (1)$$

($r = 0.976$; $n = 4$)

The correlation shown in Fig. 2 indicates a good

Scheme 5. $\Delta G_{R_1-N-R_2}^\ddagger$ values of compounds **5b**, **6b** and catechol derivatives **11** and **12**.

correspondence between the N → B bond strength and the ^{15}N NMR shifts which are shifted to lower frequencies with decreasing dissociation energy.

2.1. Theoretical studies of compounds **1b–6b**

The correlation between $\Delta G_{R_1-N-R_2}^\ddagger$ and the ^{15}N NMR chemical shifts suggests that there should be changes in the distribution of charge around the nitrogen atom for the set of compounds studied. A theoretical analysis was performed in order to obtain further information about these charge redistributions and about the differences in the N → B bond strengths. The reason for this analysis was to look for trends in the ionic and covalent nature of the N → B bond with the objective of establishing whether the N → B bond strength is related to the increase of charge polarization or to the degree of covalency.

The approach to obtain the mentioned trends is as follows: to get an acceptable geometry the molecules were optimized by the MNDO method [20]. It is known that MNDO geometries give a reasonable description of the X-ray results. This is the case for the molecules studied, as can be seen in Table 5.

It is interesting to note that we obtain open structures for **5b** and **6b**. In both cases the closed structures were used as a starting point for the geometry optimization. This indicates that the ground state for these molecules is the open structure, at least in the gas phase. The above results, and the fact that the NMR experiments show weaker dative bonds for **5b** and **6b** suggest that the MNDO calculations are appropriately reflecting the

Table 4
 ^{15}N NMR (CDCl_3) shifts of the free aminoalcohols **1a**, **3a** and **5a** and the (N-B)-diphenyl(2-aminoethoxy)boranes **1b–4b**^a

Compound	δ (ppm)	$^1J_{\text{NH}}$ (Hz)
1a	–346.5	—
1b	–324.1	71
2b	–322.4	72
3a	–346.6	—
3b-trans	–328.0	—
4b-trans ^b	–324.7	74
5a	–351.9	—

^a ^{15}N NMR spectra of **5b** and **6b** could not be obtained, because of the fast interchange of positions of the *N*-methyl groups at room temperature that broadens the ^{15}N NMR signal.

^b $\text{DMSO-}d_6$.

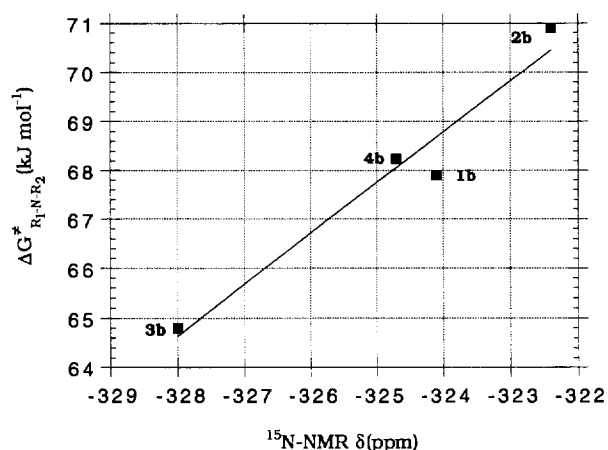


Fig. 2. Plot of ^{15}N NMR chemical shifts (ppm) vs. $\Delta G_{R_1-N-R_2}^\ddagger$ (kJ mol $^{-1}$).

Table 5
Comparison of selected calculated and measured (X-ray diffraction) bond lengths and angles of compounds **1b–6b**

Compound	$d(\text{B-B})$ (Å)		Ph-B-Ph (deg)		O-B-N (deg)	
	calc.	X-ray	calc.	X-ray	calc.	X-ray
1b	1.67	1.66(1)	111.26	113.5(11)	97.64	99.8(9)
	—	1.65(1)	—	114.7(11)	—	98.7(10)
2b	1.67	1.657(9)	111.30	116.5(6)	98.22	99.3(5)
	—	1.664(9)	—	114.1(6)	—	99.1(5)
3b-cis	1.72	1.68(2)	110.83	115.4(19)	96.21	99.4(10)
3b-trans	1.73	—	113.80	—	96.48	—
4b-cis	1.72	—	111.27	—	99.02	—
4b-trans ^a	—	1.66(1)	—	115.3(7)	—	100.6(6)
5b	open	1.744(8)	120.06	113.6(5)	—	99.1(4)
6b	open	1.74(1)	120.00	112.6(9)	—	99.1(8)

^a The MNDO calculation of **4b-trans** did not provide an appropriate geometry.

Table 6
Population analysis of the N-B bond of compounds **1b–4b**

Compound	MP bond order N-B
1b	0.1634
2b	0.1577
3b-cis	0.2114
3b-trans	0.1982
4b-cis	0.2198

Table 7
Calculated (MNDO and single point RHF/3-21G^{*}) electrostatic charges of B, N and O

Compound	Electrostatic charge			Electrostatic charge difference B-N
	B	N	O	
1b	0.48	-0.31	-0.70	0.79
2b	0.39	-0.12	-0.68	0.51
3b-cis	0.44	-0.09	-0.66	0.53
3b-trans	0.43	+0.04	-0.67	0.39
4b-cis	0.40	-0.03	-0.63	0.43
5b	0.85	-0.56	-0.59	—
6b	0.85	-0.41	-0.65	—

main interaction in these systems. The N \rightarrow B bond lengths for **1b–4b** increase as expected with decreasing ΔG^\ddagger values (**1b** \rightarrow **3b**, and **2b** \rightarrow **4b**).

Having obtained the MNDO geometry, ab initio calculations were performed at the RHF/3-21G^{*} level. All calculations were performed with the GAUSSIAN92 package.²

We selected the 3-21G^{*} basis set following two main guidelines. First there is evidence that the use of polarization functions is required to describe appropriately the boron atom environments.³ Second, we wanted to use a split-valence basis set, because this kind of basis gives a better description of charge distributions [22].

The behaviour of the covalent strength of the N \rightarrow B bond was analyzed first. In Table 6 the bond order calculated through the Mulliken population analysis [23] is displayed. It can be seen that the bond order increases with the introduction of one methyl group on the nitrogen atom (**1b** \rightarrow **3b** and **2b** \rightarrow **4b**).

The quantity to measure the degree of the ionic character of the N \rightarrow B bond interaction was the difference between the electrostatic charges [24] of the boron and the nitrogen atoms. The electrostatic charges were used, because it has been argued that these values best describe the real situation in ionic molecules [24].

Table 7 resumes the results of the calculated charges of the boron, nitrogen and oxygen atoms. The values indicate that the electrostatic charge difference between the boron and the nitrogen atoms diminishes with the introduction of a methyl group on the nitrogen atom (**1b** \rightarrow **3b**) and (**2b** \rightarrow **4b**). This coincides with the increase of the covalent character of the N \rightarrow B bond in the same direction. These results seem to indicate that the N \rightarrow B bond strength is related to the electrostatic charge difference and the polarization along this bond. However, further studies will be necessary and are in progress in order to consider also the influence of steric effects [25].

Comparing the electrostatic charge of the nitrogen atom with the ^{15}N NMR displacements (Table 4) it can be seen that an increase of the positive character of the nitrogen charge causes a shift of the ^{15}N NMR signal to lower frequencies (**1b** \rightarrow **3b** and **2b** \rightarrow **4b**), thus confirming that there exists a relationship between the ^{15}N NMR chemical shifts and the charge around the nitrogen atom.

² The structures were edited by use of SPARTAN (version 3.1, Wavefunction Inc., 18401 Van Karman Avenue, Suite 370, Irvine, CA 92715, USA) and calculated with GAUSSIAN92 (Gaussian Inc., Carnegie Office Park, Bldg 6, Pittsburgh, PA 15106, USA). The electrostatic charge was calculated with SPARTAN.

³ It has been observed that for BH_2R , BHR_2 , BR_3 (R = OH, NH_2 and CH_3) the description of the boron environment requires polarized functions [21].

2.2. X-ray crystallography of compounds **1b–6b**

Single crystals of compounds **1b–6b** have been studied by X-ray crystallography. This series of structures permits for the first time the direct comparison of structural changes with the introduction of one or two methyl groups on the nitrogen atom in (N–B)-(2-aminoethoxy)borane derivatives. To obtain these results we have included in this report all X-ray structural data, including those of lower quality. In the cases of **1b** and

Table 8
Fractional atomic coordinates for compound C₂₁H₂₂BNO (**1b**)

Atom	x	y	z	U _{iso}
O(1)	0.2417(8)	0.5937(5)	0.5942(7)	0.062(2)
O(51)	0.2353(7)	0.1314(4)	1.2724(6)	0.049(2)
N(3)	0.493(1)	0.5732(6)	0.6215(9)	0.060(3)
N(53)	-0.0129(9)	0.1102(5)	1.2453(8)	0.052(3)
B(2)	0.350(1)	0.5520(8)	0.681(1)	0.047(4)
B(52)	0.140(2)	0.0657(9)	1.271(1)	0.054(4)
C(4)	0.449(1)	0.6090(8)	0.507(1)	0.075(4)
C(5)	0.310(1)	0.6466(7)	0.525(1)	0.064(3)
C(6)	0.217(2)	0.6699(9)	0.409(1)	0.080(4)
C(7)	0.119(2)	0.6290(9)	0.348(1)	0.094(5)
C(8)	0.036(2)	0.650(1)	0.225(2)	0.113(6)
C(9)	0.063(2)	0.714(1)	0.193(2)	0.125(7)
C(10)	0.167(2)	0.764(1)	0.245(2)	0.134(7)
C(11)	0.248(2)	0.740(1)	0.360(2)	0.118(6)
C(12)	0.432(2)	0.5491(9)	0.401(1)	0.093(5)
C(13)	0.324(1)	0.4652(7)	0.673(1)	0.060(3)
C(14)	0.426(2)	0.411(1)	0.725(1)	0.095(5)
C(15)	0.396(2)	0.333(1)	0.724(2)	0.107(6)
C(16)	0.270(2)	0.309(1)	0.668(2)	0.110(6)
C(17)	0.169(2)	0.358(1)	0.616(1)	0.093(5)
C(18)	0.196(1)	0.4329(8)	0.617(1)	0.072(4)
C(19)	0.365(1)	0.5848(6)	0.820(1)	0.048(3)
C(20)	0.330(1)	0.5430(8)	0.915(1)	0.070(4)
C(21)	0.325(2)	0.5745(9)	1.031(1)	0.089(5)
C(22)	0.364(2)	0.646(1)	1.053(1)	0.090(5)
C(23)	0.402(2)	0.6914(9)	0.964(1)	0.088(5)
C(24)	0.400(1)	0.6595(8)	0.848(1)	0.075(4)
C(54)	0.017(1)	0.1887(8)	1.208(1)	0.064(4)
C(55)	0.170(1)	0.1830(7)	1.185(1)	0.060(3)
C(56)	0.256(1)	0.2564(7)	1.193(1)	0.062(4)
C(57)	0.314(1)	0.2824(8)	1.307(1)	0.070(4)
C(58)	0.401(2)	0.349(1)	1.315(1)	0.096(5)
C(59)	0.417(2)	0.383(1)	1.209(2)	0.107(6)
C(60)	0.366(2)	0.357(1)	1.094(1)	0.091(5)
C(61)	0.279(1)	0.2908(8)	1.088(1)	0.074(4)
C(62)	-0.009(2)	0.2435(9)	1.308(1)	0.092(5)
C(63)	0.169(1)	0.0245(7)	1.399(1)	0.056(3)
C(64)	0.176(1)	0.0644(8)	1.508(1)	0.076(4)
C(65)	0.201(2)	0.029(1)	1.627(1)	0.093(5)
C(66)	0.219(2)	-0.044(1)	1.630(2)	0.099(5)
C(67)	0.215(2)	-0.087(1)	1.531(2)	0.099(5)
C(68)	0.188(1)	-0.0522(8)	1.410(1)	0.077(4)
C(69)	0.145(1)	0.0118(7)	1.152(1)	0.052(3)
C(70)	0.040(1)	-0.0424(8)	1.114(1)	0.069(4)
C(71)	0.047(1)	-0.0903(9)	1.013(1)	0.085(5)
C(72)	0.164(2)	-0.0897(9)	0.959(1)	0.091(5)
C(73)	0.267(1)	-0.0362(9)	0.992(1)	0.081(4)
C(74)	0.259(1)	0.0122(8)	1.088(1)	0.063(3)

Table 9
Fractional atomic coordinates for compound C₂₁H₂₂BNO (**2b**)

Atom	x	y	z	U _{eq}
O(1)	0.2055(4)	0.5400(2)	0.4290(2)	0.0438
O(51)	-0.2898(5)	0.4595(2)	0.4297(2)	0.0508
N(3)	-0.0461(5)	0.5471(3)	0.4459(2)	0.0466
N(53)	-0.5402(5)	0.4442(3)	0.4476(2)	0.0468
B(2)	0.1035(9)	0.5217(4)	0.4815(4)	0.0445
B(52)	-0.394(1)	0.4784(5)	0.4812(4)	0.0523
C(4)	-0.0058(7)	0.5788(4)	0.3818(3)	0.0524
C(5)	0.1522(7)	0.5975(3)	0.3907(3)	0.0466
C(6)	0.2318(8)	0.6028(4)	0.3287(3)	0.0507
C(7)	0.302(1)	0.6673(4)	0.3131(4)	0.0750
C(8)	0.386(1)	0.6688(6)	0.2585(5)	0.1042
C(9)	0.397(1)	0.6112(8)	0.2196(4)	0.0995
C(10)	0.324(1)	0.5491(5)	0.2327(4)	0.0856
C(11)	0.2406(8)	0.5458(4)	0.2863(4)	0.0742
C(12)	-0.0984(9)	0.6410(5)	0.3620(4)	0.0804
C(13)	0.1205(7)	0.5699(4)	0.5446(3)	0.0462
C(14)	0.0165(8)	0.5745(4)	0.5926(4)	0.0654
C(15)	0.031(1)	0.6141(5)	0.6483(4)	0.0741
C(16)	0.152(1)	0.6538(5)	0.6585(4)	0.0778
C(17)	0.259(1)	0.6489(4)	0.6134(4)	0.0769
C(18)	0.2424(8)	0.6098(4)	0.5581(3)	0.0598
C(19)	0.1138(8)	0.4354(4)	0.4915(3)	0.0477
C(20)	0.0780(8)	0.3876(4)	0.4450(3)	0.0632
C(21)	0.100(1)	0.3139(4)	0.4513(4)	0.0743
C(22)	0.161(1)	0.2904(4)	0.5078(4)	0.0832
C(23)	0.198(1)	0.3349(5)	0.5537(4)	0.0804
C(24)	0.1725(9)	0.4087(4)	0.5494(3)	0.0639
C(54)	-0.4857(7)	0.3970(3)	0.3950(3)	0.0498
C(55)	-0.3587(7)	0.4394(3)	0.3721(3)	0.0520
C(56)	-0.2573(7)	0.4001(4)	0.3277(3)	0.0501
C(57)	-0.2096(9)	0.3329(4)	0.3406(3)	0.0677
C(58)	-0.114(1)	0.2972(4)	0.2999(5)	0.0893
C(59)	-0.064(1)	0.3328(6)	0.2480(4)	0.0798
C(60)	-0.107(1)	0.4015(6)	0.2327(4)	0.0923
C(61)	-0.2057(9)	0.4351(4)	0.2749(4)	0.0738
C(62)	-0.5932(9)	0.3769(4)	0.3436(4)	0.0757
C(63)	-0.4058(8)	0.5622(4)	0.4907(4)	0.0524
C(64)	-0.4499(8)	0.6091(4)	0.4391(4)	0.0608
C(65)	-0.444(1)	0.6823(5)	0.4445(4)	0.0803
C(66)	-0.396(1)	0.7162(4)	0.4976(6)	0.0918
C(67)	-0.352(1)	0.6729(5)	0.5510(5)	0.0946
C(68)	-0.3569(9)	0.5983(4)	0.5436(4)	0.0679
C(69)	-0.3661(8)	0.4339(4)	0.5477(3)	0.0536
C(70)	-0.2486(8)	0.3906(4)	0.5541(4)	0.0596
C(71)	-0.2247(9)	0.3527(4)	0.6120(4)	0.0742
C(72)	-0.316(1)	0.3588(5)	0.6621(4)	0.0815
C(73)	-0.434(1)	0.4008(6)	0.6561(4)	0.0852
C(74)	-0.4569(8)	0.4389(4)	0.5992(4)	0.0680

2b the asymmetric unit contains two molecules providing a low parameter-to-reflections ratio, especially in the case of **2b**, that was refined anisotropically. The introduction of methyl groups on the nitrogen atom weakens the N → B bond strength. Therefore, in the cases of **3b–6b** it was difficult to obtain suitable crystals for the X-ray diffraction experiment. The number of reflections with $I > 3\sigma I$ was not sufficient in all the cases to refine the structures anisotropically. In spite of the above, the data presented are sufficiently good to

Table 10
Fractional atomic coordinates for compound C₂₂H₂₄BNO (**3b-cis**)

Atom	x	y	z	U _{iso}
O(1)	0.1809(6)	0.6186(7)	0.7247(6)	0.041(2)
N(3)	0.0305(9)	0.4984(8)	0.7888(8)	0.048(3)
B(2)	0.055(1)	0.626(1)	0.755(1)	0.035(4)
C(4)	0.151(1)	0.447(1)	0.797(1)	0.049(4)
C(5)	0.211(1)	0.511(1)	0.707(1)	0.041(4)
C(6)	0.344(1)	0.495(1)	0.703(1)	0.042(4)
C(7)	0.388(1)	0.395(1)	0.670(1)	0.058(4)
C(8)	0.510(1)	0.383(1)	0.670(1)	0.060(4)
C(9)	0.579(1)	0.464(1)	0.693(1)	0.064(4)
C(10)	0.539(1)	0.560(1)	0.725(1)	0.062(4)
C(11)	0.416(1)	0.576(1)	0.728(1)	0.047(4)
C(12)	0.206(1)	0.466(1)	0.904(1)	0.054(4)
C(13)	-0.051(1)	0.473(1)	0.875(1)	0.078(5)
C(14)	0.040(1)	0.714(1)	0.843(1)	0.044(4)
C(15)	-0.067(1)	0.738(1)	0.895(1)	0.055(4)
C(16)	-0.078(1)	0.820(1)	0.970(1)	0.066(5)
C(17)	0.012(1)	0.876(1)	0.996(1)	0.077(5)
C(18)	0.121(1)	0.860(1)	0.946(1)	0.079(5)
C(19)	0.134(1)	0.778(1)	0.872(1)	0.055(4)
C(20)	-0.023(1)	0.6456(9)	0.6474(9)	0.035(3)
C(21)	-0.149(1)	0.644(1)	0.647(1)	0.063(4)
C(22)	-0.211(1)	0.662(1)	0.551(1)	0.059(4)
C(23)	-0.155(1)	0.684(1)	0.462(1)	0.072(5)
C(24)	-0.036(1)	0.694(1)	0.461(1)	0.064(4)
C(25)	0.030(1)	0.671(1)	0.552(1)	0.042(4)

Table 12
Fractional atomic coordinates for compound C₂₃H₂₆BNO (**5b**)

Atom	x	y	z	U _{eq}
O(1)	-0.0741(3)	0.5020(3)	0.3443(3)	0.0418
B(2)	-0.1966(6)	0.5348(5)	0.3624(5)	0.0406
N(3)	-0.2260(4)	0.5916(3)	0.2444(3)	0.0415
C(4)	-0.1064(5)	0.5893(4)	0.1919(4)	0.0401
C(5)	-0.0532(5)	0.4914(5)	0.2390(4)	0.0413
C(6)	0.0780(5)	0.4786(4)	0.2172(5)	0.0417
C(7)	0.1608(5)	0.4937(5)	0.2911(5)	0.0544
C(8)	0.2798(6)	0.4860(6)	0.2692(7)	0.0671
C(9)	0.3141(6)	0.4603(5)	0.1712(7)	0.0632
C(10)	0.2325(7)	0.4449(5)	0.0958(6)	0.0650
C(11)	0.1144(6)	0.4522(5)	0.1194(5)	0.0588
C(12)	-0.0345(6)	0.6867(5)	0.2115(5)	0.0584
C(13)	-0.2758(6)	0.6990(5)	0.2499(5)	0.0540
C(14)	-0.0929(6)	0.6459(5)	0.5026(5)	0.0483
C(15)	-0.1980(5)	0.6190(4)	0.4543(4)	0.0403
C(16)	-0.3076(5)	0.5302(5)	0.1803(4)	0.0470
C(17)	-0.0888(6)	0.7104(5)	0.5880(5)	0.0553
C(18)	-0.1918(8)	0.7517(5)	0.6274(5)	0.0596
C(19)	-0.2963(7)	0.7266(5)	0.5804(5)	0.0550
C(20)	-0.2989(6)	0.6620(5)	0.4958(4)	0.0489
C(21)	-0.2802(6)	0.4367(4)	0.3827(4)	0.0423
C(22)	-0.4035(6)	0.4385(5)	0.3927(5)	0.0548
C(23)	-0.4672(6)	0.3485(7)	0.4171(6)	0.0653
C(24)	-0.4093(8)	0.2546(6)	0.4340(6)	0.0761
C(25)	-0.2910(7)	0.2504(5)	0.4254(6)	0.0685
C(26)	-0.2253(6)	0.3406(5)	0.4021(5)	0.0557

Table 11
Fractional atomic coordinates for compound C₂₄H₃₀BNO₂ (**4b-trans**)

Atom	x	y	z	U _{iso}
O(1)	0.7074(7)	0.2206(6)	0.1337(6)	0.054(1)
B(2)	0.573(1)	0.2760(6)	0.038(1)	0.051(2)
N(3)	0.3815(8)	0.2210(4)	0.0275(6)	0.051(2)
C(4)	0.451(1)	0.1355(5)	0.0743(9)	0.051(2)
C(5)	0.614(1)	0.1586(5)	0.1973(9)	0.050(2)
C(6)	0.731(1)	0.0857(5)	0.2531(9)	0.051(2)
C(7)	0.728(1)	0.0546(6)	0.390(1)	0.069(3)
C(8)	0.832(2)	-0.0148(7)	0.445(1)	0.086(3)
C(9)	0.941(1)	-0.0509(7)	0.363(1)	0.082(3)
C(10)	0.947(1)	-0.0235(7)	0.228(1)	0.078(3)
C(11)	0.839(1)	0.0477(6)	0.170(1)	0.059(2)
C(12)	0.305(1)	0.0789(6)	0.117(1)	0.070(3)
C(13)	0.249(1)	0.2191(7)	-0.116(1)	0.072(3)
C(14)	0.622(1)	0.2851(5)	-0.1219(9)	0.048(2)
C(15)	0.553(1)	0.3491(6)	-0.216(1)	0.061(2)
C(16)	0.583(1)	0.3524(6)	-0.358(1)	0.076(3)
C(17)	0.686(1)	0.2935(6)	-0.407(1)	0.071(3)
C(18)	0.757(1)	0.2304(6)	-0.319(1)	0.067(2)
C(19)	0.727(1)	0.2256(6)	-0.1754(9)	0.064(2)
C(20)	0.551(1)	0.3632(5)	0.1215(9)	0.057(2)
C(21)	0.384(1)	0.3999(7)	0.130(1)	0.080(3)
C(22)	0.377(2)	0.4768(8)	0.205(1)	0.088(3)
C(23)	0.531(2)	0.5125(8)	0.273(1)	0.093(3)
C(24)	0.695(2)	0.4800(8)	0.266(1)	0.102(4)
C(25)	0.709(1)	0.4051(7)	0.189(1)	0.082(3)
O(2)	0.0889(8)	0.2490(4)	0.2040(6)	0.063(2)
C(26)	0.131(2)	0.2730(8)	0.355(1)	0.106(4)
C(27)	0.172(2)	0.2047(9)	0.453(1)	0.120(4)

Table 13
Fractional atomic coordinates for compound C₂₃H₂₆BNO (**6b**)

Atom	x	y	z	U _{iso}
O(1)	0.1652(7)	0.9898(7)	0.2753(9)	0.044(2)
B(2)	0.097(1)	1.0501(8)	0.393(2)	0.046(3)
N(3)	0.1673(9)	1.0089(5)	0.626(1)	0.042(2)
C(4)	0.195(1)	0.9197(6)	0.573(1)	0.040(3)
C(5)	0.257(1)	0.9287(6)	0.385(1)	0.039(3)
C(6)	0.262(1)	0.8483(6)	0.276(1)	0.035(2)
C(7)	0.130(1)	0.8093(7)	0.178(2)	0.049(3)
C(8)	0.133(1)	0.7320(8)	0.080(2)	0.067(4)
C(9)	0.272(2)	0.6933(8)	0.088(2)	0.074(4)
C(10)	0.399(1)	0.7302(8)	0.184(2)	0.070(4)
C(11)	0.395(1)	0.8069(7)	0.277(2)	0.053(3)
C(12)	0.296(1)	0.8668(8)	0.734(2)	0.070(4)
C(13)	0.062(1)	1.0100(7)	0.766(2)	0.059(3)
C(14)	0.308(1)	1.0523(8)	0.724(2)	0.060(3)
C(15)	-0.085(1)	1.0425(7)	0.340(1)	0.047(3)
C(16)	-0.155(1)	0.9873(7)	0.199(1)	0.049(3)
C(17)	-0.313(1)	0.9786(8)	0.143(2)	0.064(3)
C(18)	-0.402(1)	1.0256(8)	0.232(2)	0.066(4)
C(19)	-0.343(2)	1.0856(9)	0.369(2)	0.079(4)
C(20)	-0.181(1)	1.0935(8)	0.427(2)	0.062(3)
C(21)	0.155(1)	1.1452(6)	0.375(1)	0.037(2)
C(22)	0.128(1)	1.2154(7)	0.487(2)	0.060(3)
C(23)	0.181(1)	1.2966(8)	0.460(2)	0.060(3)
C(24)	0.260(1)	1.3096(8)	0.318(2)	0.059(3)
C(25)	0.288(1)	1.2450(8)	0.201(2)	0.067(4)
C(26)	0.241(1)	1.1638(7)	0.236(2)	0.049(3)

Table 14
Selected bond lengths (Å) for compounds **1b–6b**

Bond	1b	2b	3b-cis	4b-trans	5b	6b
B–O	1.48(1)	1.487(8)	1.49(1)	1.49(1)	1.477(7)	1.47(1)
	1.48(2)	1.492(9)				
N–B	1.66(2)	1.657(9)	1.681(2)	1.66(1)	1.744(8)	1.74(1)
	1.64(2)	1.664(9)				
C ₅ –O	1.43(1)	1.421(7)	1.40(1)	1.412(8)	1.407(6)	1.39(1)
	1.40(1)	1.407(7)				
C ₄ –N	1.41(2)	1.496(8)	1.52(2)	1.50(1)	1.525(7)	1.49(1)
	1.50(2)	1.487(8)				
C ₄ –C ₅	1.54(2)	1.539(9)	1.55(2)	1.54(1)	1.531(8)	1.53(1)
	1.53(2)	1.509(1)				

Table 15
Selected bond angles (deg) for compounds **1b–6b**

Bond	1b	2b	3b-cis	4b-trans	5b	6b
N–B–O	99.89(9)	99.3(5)	99.4(19)	100.2(6)	99.1(4)	99.1(8)
	98.7(10)	99.1(5)				
C–B–C	113.5(11)	116.5(6)	115.4(10)	115.3(7)	113.6(5)	112.6(9)
	114.7(11)	114.1(6)				
B–O–C ₅	109.7(9)	110.4(5)	109.8(10)	110.4(6)	110.2(4)	114.8(7)
	107.8(9)	111.1(5)				
B–N–C ₄	108.0(9)	106.7(5)	105.8(9)	103.5(6)	102.8(4)	99.8(7)
	106.8(9)	104.1(5)				
N–C ₄ –C ₅	102.7(10)	103.2(5)	97.5(9)	99.7(6)	100.8(4)	103.6(7)
	102.5(10)	101.2(5)				
O–C ₅ –C ₄	105.2(11)	103.8(5)	105.6(10)	103.6(6)	104.4(4)	104.2(8)
	105.2(10)	103.8(5)				

allow discussion of the changes in the N → B bond length, the N–B–O bond angle, the Ph–B–Ph bond angle and the dihedral angles in the heterocyclic rings.

Listings of fractional atomic coordinates for **1b–6b** are given in Tables 8–13 respectively; selected bond lengths for **1b–6b** and selected bond angles for **1b–6b** are given in Tables 14 and 15 respectively.

The X-ray structures of compounds **1b–6b** (Figs. 3

and 4) show the existence of intramolecular N → B bonds. Having in mind that compounds **5b** and **6b** show a weak N → B bond in NMR spectroscopy and none in theoretical calculations, it can be concluded that in the crystal-lattice there might exist additional electrostatic forces, which are able to stabilize the N → B bond. The five-membered boronate rings have twisted conforma-

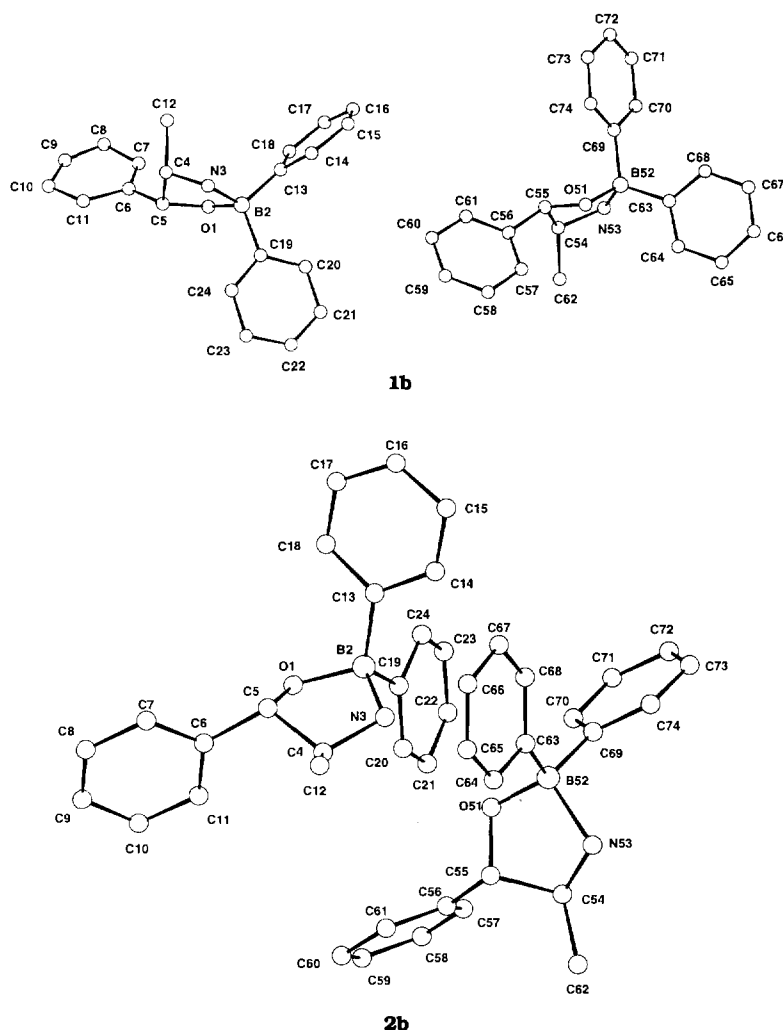
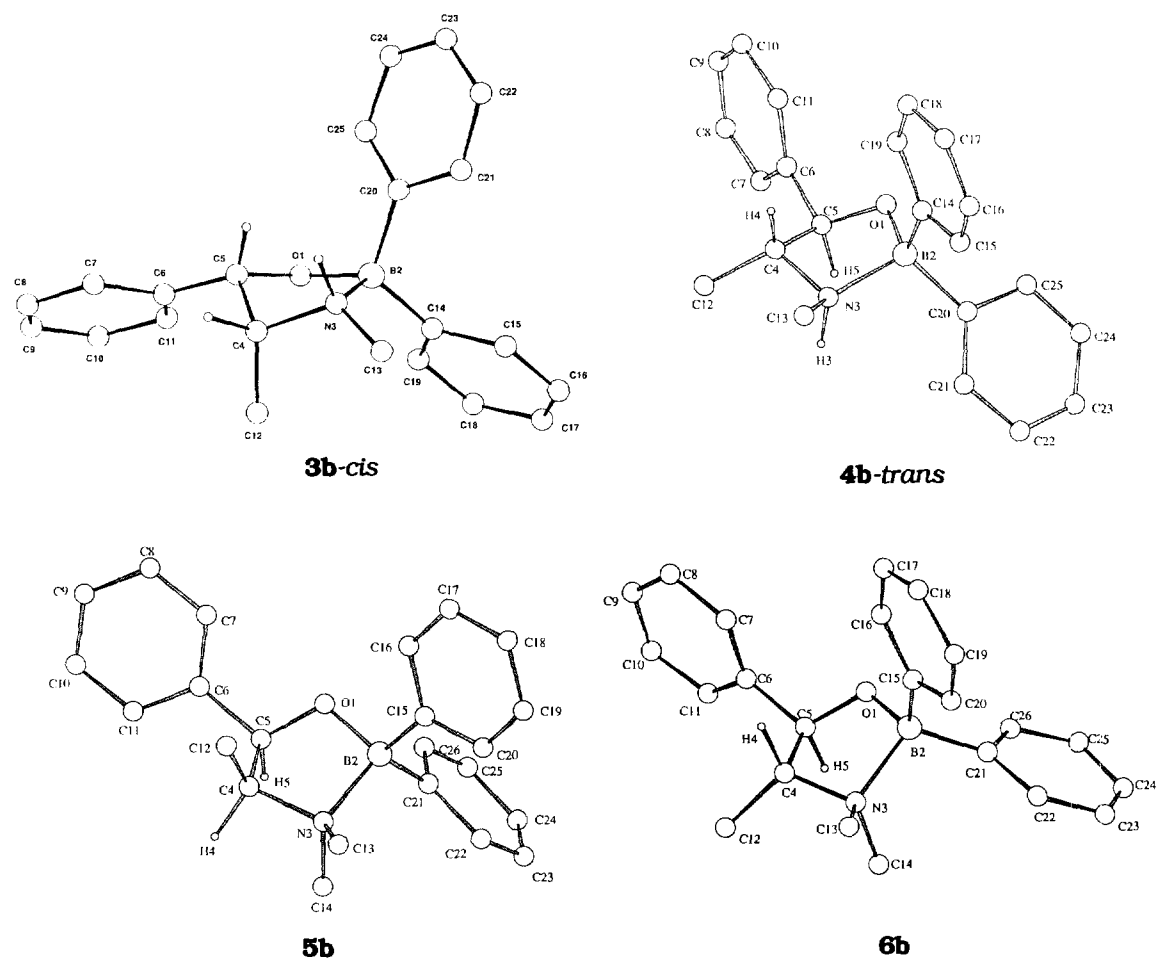


Fig. 3. Perspective views of the molecular structures of **1b** and **2b**.

Fig. 4. Perspective views of the molecular structures of **3b–6b**.

tions. The C_4 atoms are displaced out of the boronate plane by 0.496 and -0.328 Å for **1b**, 0.421 and 0.609 Å for **2b**, 0.635 Å for **3b-cis**, 0.666 Å for **4b-trans**, -0.585 Å for **5b** and -0.627 Å for **6b** in order to avoid an eclipsed conformation along the highly substituted C_4-C_5 and C_4-N bonds.

The $N \rightarrow B$ bonds in **1b** (1.66(2) and 1.64(2) Å), **2b** (1.657(9) and 1.664(9) Å), **3b-cis** (1.68(2) Å) and **4b-trans** (1.66(1) Å) are significantly shorter than those in **5b** (1.744(8) Å) and **6b** (1.74(1) Å), in accord with the decreasing $N \rightarrow B$ bond stability. The $B-O$ bond is not

significantly different in the three compounds. The data for **1b–6b** obtained in this study are in agreement with that available in the literature [4–7,26], where it has been reported that $N \rightarrow B$ bond distances in (2-aminoethoxy)borane compounds are in the range of 1.638 to 1.759 Å, depending on the basicity of the amine ligands. In those cases, where the basicity of the nitrogen atom which coordinates to the boron atom is not strong, the distance is longer, in the range of 1.74–1.76 Å.

The $N-B-O$ bond angles lie in the expected range of

Table 16

Dihedral angles (deg) at the heterocyclic ring with steric interactions between the ring substituents for compounds **1b–6b**

Dihedral angle	1b	2b	3b-cis	4b-trans	5b	6b
$C(12)-C(4)-C(5)-C(6)$	-44.47 -37.58	-78.93 -67.13	52.35 —	66.00 —	-47.71 —	66.27 —
$C(13)-N(3)-C(4)-C(12)$	—	—	-51.36	-69.36	33.17	-72.9
$C(14)-B(2)-N(3)-C(13)$	—	—	28.66	-24.29	—	—
$C(15)-B(2)-N(3)-C(13)$	—	—	—	—	-14.40	-25.67
$C(21)-B(2)-N(3)-C(14)$	—	—	—	—	-8.76	-23.84
$C(14)-N(3)-C(4)-C(12)$	—	—	—	—	—	46.63

98–100° and the Ph–B–Ph angles are in the range of 112–117° (Table 15). The crystal structure of **4b-trans** shows an OH–O hydrogen bond with an ethanol molecule.

Based on the study of Toyota and Ōki, who found that the magnitude of the tetrahedral character (THC) of the boron atom can be correlated with the strength of the N → B bond [7], we calculated the tetrahedral character for compounds **1b–6b** and correlated these values with the $\Delta G_{R1-N-R2}^\ddagger$ values of the N → B bond, but no correlation was found. This may be due to the presence of the two bulky phenyl groups at the boron atom.

Table 16 summarizes the dihedral angles at the heterocyclic rings of compounds **1b–6b**, showing the steric interactions between the substituents. Compounds **1b** and **2b** show one steric interaction, **3b** and **4b** three, **5b** four, and compound **6b** five. On the other hand, a comparison of the corresponding ΔG^\ddagger values (Table 3) shows that compound **6b** has a lower value than **2b**, **3b** and **4b** (less steric interactions). This is evidence that steric effects play an important role in the ΔG^\ddagger values.

3. Conclusions

The present study has shown that the N → B bond stability in the (N–B)-diphenyl(2-aminoethoxy)boranes **1b–6b** decreases significantly when the nitrogen atom is substituted by two methyl groups, while substitution by one methyl group seems to be of less importance. The N → B bond is stronger when the substituents along the C₄–C₅ bond are in a *trans* configuration (pseudoephedrine derivatives ↔ ephedrine derivatives). Therefore, in order to synthesize (N–B)-(2-aminoethoxy)boranes with strong N → B bonds, it has to be considered that steric effects along the whole five-membered heterocyclic ring influence significantly the N → B bond strength and should be avoided, where possible.

4. Experimental

The ¹H-, ¹³C- and ¹¹B-NMR spectra were recorded using Varian EM-390, Jeol FX90 and Jeol GSX-270 spectrometers. Chemical shifts (parts per million) are relative to BF₃–Et₂O and (CH₃)₄Si. Coupling constants are quoted in hertz. The ¹⁵N NMR spectra were recorded at the natural abundance level with a Jeol GXS-270 spectrometer operating at 27.25 MHz using a multinuclear 5 mm probe and the refocused INEPT pulse sequence to detect the ¹⁵N NMR signal. Diphenylborinic acid was prepared from the corresponding ethanolamine complex as described in the literature [27].

4.1. General procedure

A solution of the aminoalcohol in methanol was treated with a 10% excess of diphenylborinic acid and the mixture was heated under reflux for 1 h. The solution was evaporated to dryness and the crude product crystallized.

4.2. (N–B)-Diphenyl(1-(R)-phenyl-2-(S)-methyl-2-aminoethoxy)borane (**1b**)

Norephedrine (1 g, 6.6 mmol) and diphenylborinic acid (1.3 g, 7.2 mmol). Compound **1b** was first crystallized from acetone–hexane followed by recrystallization from ethyl acetate–hexane (0.25 g, 12%); m.p. 189–191 °C; ν_{\max} (KBr): 2656, 1432, 1151 cm⁻¹; δ_{H} (270 MHz; CDCl₃): 0.62 (d, *J* = 6.6 Hz, 3H, C₄–CH₃), 3.28 (m, 1H, H₄), 3.86 (br, 2H, NH), 4.98 (d, *J* = 5.3 Hz, 1H, H₅), 7.15–7.57 (m, 15H, arom.) ppm; δ_{C} (67.8 MHz, CDCl₃): 16.0 (C–CH₃), 54.4 (C₄), 77.9 (C₅), C- ϕ (126.3 (*o*), 127.2 (*p*), 128.2 (*m*), 140.1 (*i*)), B- ϕ (126.3 (*p*), 126.6 (*p*), 127.6 (*m*), 127.8 (*m*), 131.4 (*o*), 132.0 (*o*), 148.9 (*i*, *br*), 149.7 (*i*, *br*)) ppm; δ_{B} (28.69 MHz, CDCl₃): +7.4 ppm; *m/z*: 315 (M⁺, 1), 314 (M⁺ – 1, 2), 239 (5), 238 (35), 237 (11), 222 (5), 208 (14), 182 (5), 165 (7), 134 (24), 117 (10), 105 (23), 104 (11), 91 (13), 90 (7), 89 (6), 79 (5), 78 (19), 77 (12), 57 (8), 56 (6), 55 (8), 51 (11), 50 (6), 45 (6), 44 (100), 43 (10), 42 (8), 41 (7), 39 (6), 29 (6), 27 (5), 18 (26), 17 (6).

4.3. (N–B)-Diphenyl(1-(R)-phenyl-2-(R)-methyl-2-aminoethoxy)borane (**2b**)

Norpseudoephedrine (1 g, 6.6 mmol) and diphenylborinic acid (1.3 g, 7.2 mmol). Compound **2b** was crystallized from a mixture of methanol and diethyl ether (1.5 g, 72%); m.p. 209–214 °C; ν_{\max} (KBr): 2820, 1598, 1432, 1155, 1059 cm⁻¹; δ_{H} (270 MHz, CDCl₃): 1.12 (d, *J* = 6.6 Hz, 3H, C₄–CH₃), 3.00 (m, 1H, H₄), 4.12 (br, 2H, NH), 4.49 (d, *J* = 9.2 Hz, 1H, H₅), 7.19–7.56 (m, 15H, arom.) ppm; δ_{C} (67.8 MHz, CDCl₃): 16.3 (C–CH₃), 59.1 (C₄), 83.0 (C₅), C- ϕ (127.8 (*o*), 128.1 (*p*), 128.6 (*m*), 140.8 (*i*)), B- ϕ (126.3 (*p*), 126.7 (*p*), 127.0 (*m*), 127.6 (*m*), 131.4 (*o*), 132.3 (*o*), 149.4 (br, *i*)) ppm; δ_{B} (28.69 MHz, CDCl₃): +7.0 ppm; *m/z*: 315 (M⁺, 6), 314 (M⁺ – 1, 9), 239 (17), 238 (100), 237 (34), 236 (5), 222 (10), 221 (5), 208 (10), 195 (21), 167 (6), 165 (12), 163 (9), 160 (9), 137 (5), 135 (86), 134 (60), 119 (5), 118 (12), 117 (33), 115 (13), 105 (17), 104 (16), 103 (6), 91 (27), 90 (13), 89 (12), 78 (7), 77 (19), 56 (9), 52 (5), 51 (17), 50 (5), 44 (87), 42 (9), 39 (5), 28 (8), 18 (18).

4.4. (N–B)-Diphenyl[N-(R,S)-methyl-(1-(R)-phenyl-2-(S)-methyl-2-aminoethoxy)]borane (**3b-trans** and **3b-cis**)

Ephedrine (1 g, 6.0 mmol) and diphenylborinic acid (1.2 g, 6.6 mmol). Compound **3b-cis** was crystallized

from ethanol–acetone, (1.4 g, 70%); m.p. 242–245 °C, ν_{\max} (KBr): 2681, 1432, 1151, 1024 cm^{-1} ; δ_{H} (270 MHz, CDCl_3): 0.83 (d, $J = 6.6$ Hz, 3H, $\text{C}_4\text{-CH}_3$), 2.53 (s, 3H, N- CH_3), 3.48 (m, 1H, H_4), 3.90 (br, 1H, NH), 5.49 (d, 5.9 Hz, 1H, H_5), 7.09–7.65 (m) ppm; δ_{C} (67.8 MHz, CDCl_3): 13.4 ($\text{C}_4\text{-CH}_3$), 34.4 (N- CH_3), 61.7 (C_4), 78.4 (C_5), C- ϕ (126.4 (p), 126.7 (o), 127.4 (m), 141.0 (i)), B- ϕ (127.6 (p), 128.3 (m), 131.9 (o), 133.0 (o), 148.0 (br, i)) ppm; δ_{B} (28.69 MHz, CDCl_3): +5.0 ppm; m/z : 329 (M^+ , 5), 328 ($\text{M}^+ - 1$, 9), 253 (17), 252 (100), 251 (30), 236 (10), 182 (8), 176 (10), 174 (5), 165 (6), 149 (7), 148 (51), 133 (8), 132 (18), 131 (6), 118 (9), 117 (16), 115 (16), 105 (18), 104 (23), 103 (8), 91 (19), 90 (7), 89 (7), 79 (5), 78 (38), 77 (20), 76 (5), 59 (5), 58 (80), 56 (11), 53 (6), 52 (10), 51 (18), 50 (10), 44 (8), 43 (8), 42 (8), 39 (8), 30 (12), 29 (5), 27 (5).

4.5. (*N-B*)-Diphenyl[*N*-(*S*)-methyl-(1-(*R*)-phenyl-2-(*R*)-methyl-2-aminoethoxy)]borane (**4b-trans**)

Pseudoephedrine (1 g, 6.0 mmol) and diphenylborinic acid (1.29 g, 6.6 mmol). Compound **4b** was crystallized from acetone–ethanol (1.77 g, 88%); m.p. 168–170 °C, ν_{\max} (KBr): 2715, 1161, 1090 cm^{-1} ; δ_{H} (270 MHz, CDCl_3): 1.05 (d, $J = 6.6$ Hz, 3H, $\text{C}_4\text{-CH}_3$), 2.28 (d, $J = 5.9$ Hz, 3H, N- CH_3), 2.65 (m, 1H, H_4), 3.66 (br, 1H, NH), 4.44 (d, $J = 9.2$ Hz, 1H, H_5), 7.15–7.66 (m, 15H, arom.) ppm; δ_{C} (67.8 MHz, CDCl_3): 13.7 (C-

CH_3), 36.8 (N- CH_2), 68.0 (C_4), 81.7 (C_5), C- ϕ (128.1 (p), 126.9 (o), 127.6 (m), 140.8 (i)), B- ϕ (126.4 (p), 127.7 (m), 128.0 (p), 128.5 (m), 131.2 (o), 133.7 (o)) ppm; δ_{B} (28.69 MHz, CDCl_3): +8.0 ppm; m/z : 329 (M^+ , 6), 330 ($\text{M}^+ + 1$, 7), 328 ($\text{M}^+ - 1$, 6), 253 (18), 252 (100), 251 (33), 236 (9), 195 (8), 165 (6), 163 (5), 149 (9), 148 (69), 133 (12), 132 (7), 118 (19), 117 (27), 115 (10), 105 (6), 91 (34), 90 (11), 89 (11), 77 (19), 58 (57), 56 (19), 51 (20), 50 (5), 45 (12), 43 (88), 42 (15), 39 (6), 31 (29), 30 (21), 29 (13), 27 (11), 15 (5).

4.6. (*N-B*)-Diphenyl[*N,N*-dimethyl-(1-(*R*)-phenyl-2-(*S*)-methyl-2-aminoethoxy)]borane (**5b**)

N-Methylephedrine (1 g, 5.5 mmol) and diphenylborinic acid (1.1 g, 5.7 mmol). Compound **5b** was crystallized from a mixture of chloroform–hexane (1.2 g, 63%); m.p. 205–208 °C, ν_{\max} (KBr): 2600, 1431, 1166, 1025 cm^{-1} ; δ_{H} (270 MHz, CDCl_3): 0.78 (d, $J = 7.3$ Hz, 3H, $\text{C}_4\text{-CH}_3$), 2.38 (s, 3H, N- CH_3), 3.40 (m, 1H, H_4), 5.64 (d, $J = 7.9$ Hz, 1H, H_5), 7.15–7.53 (m, 15H, arom.) ppm; δ_{C} (67.8 MHz, CDCl_3): 9.6 (C- CH_3), 44.0 (N-Me), 65.2 (C_4), 76.7 (C_5), C- ϕ (127.2 (m), 128.3 (p), 127.1 (o), 141.6 (i)), B- ϕ (127.4 (m), 128.0 (m), 126.6 (p), 126.0 (p), 131.9 (o), 133.2 (o), 147.6 (i)) ppm; δ_{B} (28.69 MHz, CDCl_3): +5.5 ppm; m/z : 343 (M^+ , 4), 342 ($\text{M}^+ - 1$, 9), 267 (20), 266 (100), 265 (25), 167 (7), 165 (15), 164 (5), 163 (11), 162 (16), 105

Table 17
Crystal data of compounds **1b–6b**

Compound	1b ^{a,b}	2b ^{a,b}	3b-cis ^{a,b}	4b-trans ^{a,c}	5b ^{a,c}	6b ^{a,c}
Formula	$\text{C}_{21}\text{H}_{22}\text{BNO}$	$\text{C}_{21}\text{H}_{22}\text{BNO}$	$\text{C}_{22}\text{H}_{24}\text{BNO}$	$\text{C}_{22}\text{H}_{27}\text{BNO}_2$	$\text{C}_{23}\text{H}_{26}\text{BNO}$	$\text{C}_{21}\text{H}_{26}\text{BNO}$
Fw	315.2	315.2	329.3	329.3 ETOH	343.3	343.3
System	monoclinic	orthorhombic	orthorhombic	monoclinic	orthorhombic	monoclinic
Space group	$P2_1$	$P2_12_12_1$	$P2_12_12_1$	$P2_1$	$P2_12_12_1$	$P2_1$
a (Å)	9.572(1)	9.422(1)	11.423(7)	7.402(1)	11.386(3)	9.091(4)
b (Å)	17.808(3)	18.562(4)	12.514(2)	16.082(1)	12.910(3)	15.823(2)
c (Å)	10.981(1)	20.639(8)	12.660(12)	9.333(1)	13.112(1)	6.936(4)
β (deg)	99.49(1)	90	90	101.51(1)	90	101.84(6)
V (Å ³)	1846(2)	3609(8)	1810(1)	1088(2)	1927(2)	976(2)
Z	4	8	4	2	4	2
d_{calc} (g cm^{-3})	1.13	1.15	1.21	1.14	1.18	1.17
Scan width (deg)	$0.8 + 0.35 \tan \theta$	$0.8 + 0.35 \tan \theta$	$1.89 + 0.94 \tan \theta$	$0.8 + 0.35 \tan \theta$	$0.8 + 0.35 \tan \theta$	$1.1 + 0.35 \tan \theta$
Scan speed (deg min^{-1})	$1.5 < \text{sp.} < 20.1$	$1.1 < \text{sp.} < 20.1$	$1.8 < \text{sp.} < 20.1$	$1.8 < \text{sp.} < 20.1$	$1.8 < \text{sp.} < 20.1$	$3.0 < \text{sp.} < 12.0$
No. of reflections collected	3508	3556	1833	2116	1960	1953
No. of unique reflections	3302	3556	1814	1983	1937	1777
Merging R	0.01	—	—	0.02	—	0.04
No. of reflections with $I > 3\sigma I$	1479	1802	585	1116	1104	907
Absorption coefficient correction	$0.71 < c. < 1.17$	—	$0.85 < c. < 1.15$	$0.80 < c. < 1.07$	$0.89 < c. < 1.31$	$0.73 < c. < 1.34$
R	0.081	0.043	0.063	0.072	0.045	0.077
R_w	0.075	0.039	0.062	0.065	0.043	0.075
No. of variables	193	434	101	115	237	236

^a MoK α , scan type $\omega/2\theta$, 2θ range: $4 < 2\theta < 50^\circ$; unit weight scheme.

^b ENRAF NONIUS CAD4F.

^c PW 1100.

(10), 104 (8), 78 (16), 77 (14), 73 (6), 72 (70), 71 (5), 57(8), 56 (7), 55 (8), 53 (5), 52 (6), 51 (15), 50 (8), 44 (18), 43 (16), 42 (11), 41 (13), 39 (9), 29 (14), 28 (14), 27 (14), 26 (5), 17 (13), 16 (7), 15 (9).

4.7. (*N*-*B*)-Diphenyl[*N,N*-dimethyl-(1-(*R*)-phenyl-2-(*R*)-methyl-2-aminoethoxy)]borane (**6b**)

N-Methylpseudoephedrine (1 g, 5.5 mmol) and diphenylborinic acid (1.1 g, 6.0 mmol). Compound **6b** was crystallized from a mixture of chloroform–hexane, m.p. 226–230 °C, ν_{\max} (KBr): 2537, 1431, 1142, 1069 cm^{-1} ; δ_{H} (270 MHz, CDCl_3): 0.95 (d, $J = 6.6$ Hz, 3H, $\text{C}_4\text{-CH}_3$), 2.40 (s, 3H, N-CH_3), 3.20 (m, 1H, H_4), 4.81 (d, $J = 9.9$ Hz, 1H, H_5), 7.16–7.86 (m, 15 H, arom.) ppm; δ_{C} (67.8 MHz, CDCl_3): 8.9 (C-CH_3), 44.4 (N-CH_3), 69.4 (C_4), 80.5 (C_5), $\text{C-}\phi$ 126.3 (*p*), 127.5 (*o*), 128.5 (*m*), 141.2 (*i*), $\text{B-}\phi$ (127.2 (*m*), 128.0 (*p*), 133.4 (*o*), 147.6 (*i*)) ppm; δ_{B} (28.69 MHz, CDCl_3): +9.6 ppm; m/z : 342 (M, 3), 343 ($\text{M}^+ + 1$, 1), 341 ($\text{M}^+ - 1$, 1), 267(9), 266 (45), 265 (11), 163 (5), 162 (18), 147 (5), 117 (6), 91 (9), 77 (7), 73 (5), 72 (100), 56 (5), 51 (7), 44 (8), 42 (6).

4.8. X-ray analysis of compounds **1b–6b**

Selected crystals of **1b–6b** were set up on an automatic diffractometer. Compound **4b-trans** was sealed in a Lindemann tube. Intensity data for the six crystals were measured at room temperature. Unit cell dimensions with estimated standard deviations were obtained from least squares refinements of the setting angles of 24 well-centered reflections. Two standard reflections were monitored periodically; they showed no significant change during data collection. Crystallographic data and other pertinent information are summarized in Table 17. Corrections were made for Lorentz and polarization effects. Empirical absorption corrections (DIFABS [28]) were applied.

Computations were performed by using CRYSTALS [29] adapted on a MicroVax II. Atomic form factors for neutral C, B, O, N and H were taken from Ref. [30]. Anomalous dispersion was taken into account. The structures were solved by direct methods and subsequent Fourier maps.

With the exceptions of **1b** and **2b**, all hydrogen atoms were found on Fourier difference maps, the others were located theoretically and their positions were not refined. Non-hydrogen atoms were isotropically and, where possible anisotropically, refined, and one isotropic overall thermal parameter for the hydrogen atoms was refined. Least squares refinements were carried out by minimizing the function $\sum w(|F_o| - |F_c|)^2$, where F_o and F_c are the observed and calculated structure factors. Unit weight was used. Models reached convergence with $R = \sum(|F_o| - |F_c|)/\sum|F_o|$ and $R_w = [\sum w(|F_o| -$

$|F_c|)^2/\sum w(F_o)^2]^{1/2}$ having values listed in Table 17. Criteria for a satisfactory complete analysis were the ratios of r.m.s. shift to standard deviation being less than 0.1 and no significant features in the final difference map. In the case of **1b** with two molecules in the asymmetric unit the correlation coefficients were analyzed in order to exclude the higher symmetric space group $P2_1/m$.

Lists of the atomic parameters, bond lengths, bond angles and thermal parameters have been deposited at the Cambridge Crystallographic Data Centre.

Acknowledgements

Financial support from Conacyt is acknowledged and H.H. thanks the Secretary of Foreign Relations for a scholarship. We are grateful to Guillermo Uribe and Victor González Díaz for NMR spectra.

References

- [1] H.C. Brown, J.V.N. Vara Prasad, *J. Am. Chem. Soc.* 108 (1986) 2049. H.C. Brown, J.V.N. Vara Prasad, *J. Org. Chem.* 51 (1986) 4526.
- [2] S. Masamune, B.M. Kim, J.S. Petersen, T. Sato, S.J. Veenstra, *J. Am. Chem. Soc.* 107 (1985) 4549.
- [3] S. Toyota, M. Ōki, *Bull. Chem. Soc. Jpn.* 63 (1990) 1168. S. Toyota, M. Ōki, *Bull. Chem. Soc. Jpn.* 64 (1991) 1554. F. Santiesteban, M.A. Campos, H. Morales, R. Contreras, B. Wrackmeyer, *Polyhedron* 3 (1984) 589.
- [4] N. Farfán, P. Joseph-Nathan, L.M. Chiquete, R. Contreras, *J. Organomet. Chem.* 348 (1988) 149.
- [5] N. Farfán, T. Mancilla, D. Castillo, G. Uribe, L. Carrillo, P. Joseph-Nathan, R. Contreras, *J. Organomet. Chem.* 381 (1990) 1.
- [6] N. Farfán, D. Castillo, P. Joseph-Nathan, R. Contreras, L.V. Szentpály, *J. Chem. Soc. Perkin Trans. 2*: (1992) 527.
- [7] S. Toyota, M. Ōki, *Bull. Chem. Soc. Jpn.* 65 (1992) 1832.
- [8] G. Ferguson, J.F. Gallagher, D. Murphy, J.P. Sheehan, T.R. Spalding, *Polyhedron* 12 (1993) 859.
- [9] F. Santiesteban, T. Mancilla, A. Kláébé, R. Contreras, *Tetrahedron Lett.* 24 (1983) 759.
- [10] T. Mancilla, F. Santiesteban, R. Contreras, A. Kláébé, *Tetrahedron Lett.* 23 (1982) 759. R. Contreras, F. Santiesteban, M.A. Paz-Sandoval, B. Wrackmeyer, *Tetrahedron* 40 (1984) 3829.
- [11] M.A. Paz-Sandoval, F. Santiesteban, R. Contreras, *Magn. Reson. Chem.* 23 (1985) 428.
- [12] E.J. Corey, R.K. Bakshi, S. Shibata, *J. Am. Chem. Soc.* 109 (1987) 5551.
- [13] E.J. Corey, *Pure Appl. Chem.* 62 (1990) 1209.
- [14] E.J. Corey, M. Azimioara, S. Sarshar, *Tetrahedron Lett.* 33 (1992) 3429.
- [15] E.J. Corey, J.O. Link, *Tetrahedron Lett.* 33 (1992) 3431.
- [16] S. Wallbaum, J. Martens, *Tetrahedron Asymmetry* 3 (1992) 1475.
- [17] N. Farfán, D. Silva, R. Santillan, *J. Heteroatom. Chem.* 4 (1993) 533.
- [18] H. Friebolin, *Ein- und zweidimensionale NMR-Spektroskopie*, VCH Stuttgart, 2nd edition, 1992, p. 294.

- [19] M. Witkowski, L. Stefaniak, G.A. Webb, Annual Reports on NMR Spectroscopy, vol. 25, Academic Press, San Diego, CA, 1993, p. 70.
- [20] M. Dewar, W. Thiel, J. Am. Chem. Soc. 99 (1977) 4899.
- [21] M. Galván, J.L. Gázquez, A. Vela, R. Contreras, N. Farfán and A. Paz-Sandoval, Proc. VIII. Coloquio de la Academia Mexicana de Química Inorgánica, 1990, p. 71.
- [22] W.J. Hehre et al., Ab initio Molecular Orbital Theory, Wiley, New York, 1st edition, 1985, p. 336.
- [23] R.S. Mulliken, J. Chem Phys. 23 (1955) 1833; 1841; 2338; 2348.
- [24] L.E. Chirlian, M.M. Francl, J. Comput. Chem. 8 (1987) 894.
- [25] H. Höpfl, M. Galván, N. Farfán, R. Santillan, J. Mol. Struct. Theochem. in press.
- [26] W. Kliegel, G. Lubkowitz, S.J. Rettig, J. Trotter, Can. J. Chem. 69 (1984) 1227. W. Kliegel, S.J. Rettig, J. Trotter, Can. J. Chem. 62 (1984) 515. H. Amt, W. Kliegel, S.J. Rettig, J. Trotter, Can. J. Chem. 68 (1990) 1791. S.J. Rettig, J. Trotter, Can. J. Chem. 55 (1977) 3071. S.J. Rettig, J. Trotter, Acta Crystallogr. Sect. B: 30 (1974) 2139.
- [27] G.N. Chremos, H. Weidmann, H.K. Zimmerman, J. Org. Chem. 26 (1961) 1683.
- [28] N. Walker, D. Stuart, Acta Crystallogr. 39 (1983) 158.
- [29] D.J. Watkin, J.R. Carruthers, P.W. Betteridge, CRYSTALS, An Advanced Crystallographic Program System, Chemical Crystallography Laboratory, University of Oxford, Oxford, 1988.
- [30] International Tables for X-Ray Crystallography, vol. 4, Kynoch Press, Birmingham, UK, 1974.